Available online at www.sciencedirect.com

ScienceDirect

IFAC Papers Online CONFERENCE PAPER ARCHIVE

IFAC PapersOnLine 50-1 (2017) 1571–1576

# Identification of the non-linear dynamics and state of charge estimation of a $LiFePO_4$ battery using constrained unscented Kalman filter

**Syam Parakkadavath** * **Bharath Bhikkaji** **

* *Department of Electrical Engineering, Indian Institute of Technology Madras, Chennai, India, 600036*

** *Department of Electrical Engineering, Indian Institute of Technology Madras, Chennai, India, 600036 e-mail: (bharath@ee.iitm.ac.in).*

**Abstract:** State of charge (SOC) estimation of a $LiFePO_4$ battery exhibiting significant hysteresis is considered. The dynamics of the battery is modeled as a linear system in conjunction with a non-linear hysteresis block. The linear part is assumed to be of a second order equivalent circuit model along with an open circuit voltage (OCV) source $V_{oc}$. The circuit model is descretised and the resulting parameters are modeled as a multivariate random walk with a diagonal noise covariance matrix. These parameters are estimated using a Kalman filter. The linear model is then validated using a hybrid pulse power characterisation (HPPC) current profile. The major loop of the non-linear hysteresis relating $V_{oc}$ and SOC is experimentally determined by charging and discharging the battery with low magnitude currents. Using Chebyshev polynomials, a model is fit for the hysteresis curves. Constrained unscented Kalman filter (CUKF) is used for estimating the minor loops of the hysteresis, and the SOC. The SOC estimation is then validated from a full electrochemical model simulation of the battery using COMSOL software.



*Keywords:* Lithium ion battery, State of charge, Chebyshev polynomial, Unscented Kalman filter

## 1. INTRODUCTION

A battery management system (BMS) consists of hardware and software units that monitor and control the charging and discharging of a rechargeable battery module. The performance and health of a battery pack depends on how closely the BMS can track the state of charge (SOC) and the state of health (SOH) in real time. The SOC is defined as the ratio of charge remaining in a battery to its maximum rated capacity and SOH is a measure of the maximum attainable capacity of the battery at any point of its operational life. Since both SOC and SOH cannot be measured directly, they are estimated from measurable quantities like terminal voltage ($V_t$) and the current ($I$). The focus of this paper is SOC estimation of a $LiFePO_4$ battery exhibiting hysteresis.

A mathematical model of the battery is an integral part of any BMS software. Battery models can be broadly categorised into two groups. (i) Electrochemical models (EM), (Prada et al. (2012)), which consist of partial differential equations (PDE) characterising the dynamics of chemical reactions in the cell. (ii) Equivalent circuit models (ECM), (Lim et al. (2016)), which are electric circuits with their dynamics being equivalent to the battery dynamics.

EM can simulate the battery accurately but at the cost of heavy computations thereby making it difficult to embed in real-time applications.

In an ECM, the values of circuit elements are the parameters of the model. Parameters are dynamically varying, can be identified using recursive system identification methods. The input-output data required for the identification is obtained by passing a known current through the battery and measuring the terminal voltage response $V_t$. In general, lesser computation load, along with the ability to track the parameters in real time, makes the ECM an attractive choice for developing a BMS.

The simplest form of an ECM is a capacitor. Here the SOC can be calculated by integrating the current passing through the battery (commonly referred as coulomb counting). Though simple, the limitation of this method is the accumulation of error due to uncertainty in initial condition and loss during charging/discharging.

In this paper, the battery is modeled as a $2^{nd}$ order ECM, see Figure 1. Here, the RC blocks characterise different dynamic phenomena occurring inside the battery. The open circuit voltage $V_{oc}$ is taken as a sum of a time varying voltage $V_0$ and a voltage due to hysteresis $V_{hys}$. The circuit model is first descretised. To accommodate the time varying nature of the model parameters, they are modeled as a random walk. By taking current $I$ as input and terminal voltage $V_t$ as output, a Kalman filter is used to estimate the parameters and $V_{oc}$ from the circuit model.


10.1016/j.ifacol.2017.08.311

Certain types of Lithium ion batteries show hysteresis behavior between SOC and $V_{oc}$. In this paper, to model the hysteresis, a small but constant current (charging/discharging) is applied across the battery. At a very low magnitude of current, the terminal voltage $V_t$ of the battery is almost equal to the $V_{oc}$ and integrating the current (coulomb counting) would approximately give the SOC of the battery. The SOC and the $V_{oc}$ are plotted over one full charging and discharging cycle to obtain the major loop of the hysteresis. A polynomial is fit to the major loop, using Chebyshev polynomials. Using the polynomial fit of hysteresis major curves, a hysteresis model is developed. A constrained unscented Kalman filter (CUKF) is used to estimate the SOC from the hysteresis model.

The above mentioned SOC estimation paradigm is applied to a commercially available $LiFePO_4$ battery which is known to show notable hysteresis. A known current profile is applied across the battery and the terminal voltage $V_t$ is recorded. From the input current and output voltage data, the $V_{oc}$ is estimated using the Kalman filter and the SOC is estimated using the CUKF. To validate the SOC estimates obtained, a full electrochemical model of the battery is simulated using COMSOL for the same current profile. The experimentally verified parameters of the battery used for building the COMSOL model is available in Prada et al. (2012). This validates the effectiveness and reliability of the proposed method. SOC estimated by COMSOL is assumed to be close to actual SOC and is compared with the SOC estimated using the proposed algorithm. They are found to be in close match.

This paper is organised as follows. In Section 2, the circuit model for the Li-ion battery is discussed. Section 3 details the experimental setup. Section 4 contains the entire algorithm proposed for SOC estimation. Section 5 provides an experimental validation for the proposed algorithm. And finally, the paper concludes in Section 6.

## 2. MODELING OF LITHIUM ION BATTERY

As a trade off between minimal execution time and accuracy of the estimation, an ECM with two RC blocks is chosen to capture the linear dynamics of the battery, see Fig. 1. This is a well known model and has been used frequently in the past (Tang et al. (2011); Lim et al. (2016)). Here, the first block $R_1C_1$ characterises the diffusion of $Li+$ ions across the concentration gradient and the second block $R_2C_2$ accounts for double layer effect in the electrodes. The resistor $R$ represents the effective internal impedance of the cell. $V_{hys}$ is the voltage due to hysteresis and $V_t$ is the terminal voltage across the battery. $I$ is the current passing through the battery, which is taken as positive while discharging and negative while charging.

## 3. EXPERIMENTAL SETUP

A commercial Li-ion cell, ANR26650M1A from A123 systems is utilised for this study. The rated capacity of the cell is 2300 mAh and the nominal voltage is 3V. The voltage at fully discharged state is 2.8V and at fully charged state is 3.6V. The cathode material is $LiFePO_4$ and the anode is made of graphite. Three of such cells are connected in parallel to form a battery with an overall capacity of 6900 mAh, which is used for the experiments. A battery tester (Kikusui PFX2021, 20V, 10A) is used to procure the terminal voltage ($V_t$) and current (I) as data for all charging-discharging experiments. All measurements were taken at room temperature.

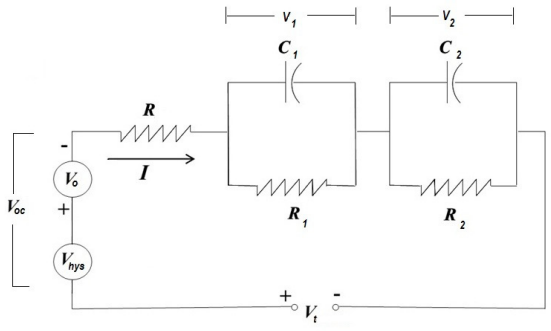


Fig. 1. Second order ECM of a Li ion battery.

## 4. ESTIMATION ALGORITHMS

There are two stages leading to SOC estimation. In the first stage, $V_{oc}$ is estimated from $V_t$ and $I$, and in the second stage the SOC is estimated from the $V_{oc}$.

### *4.1 $V_{oc}$ estimation*

From the circuit model shown in Fig. 1, using Kirchhoff law, the following relationship can be derived,

$$V_t(k) = V_{oc}(k) + I(k)R + V_1(k) + V_2(k) + e(k) \quad (1)$$

where $e(k)$ is the measurement noise. $V_1(k)$ and $V_2(k)$ are the voltages across the RC blocks. $I(k)$ is the current through the battery and $V_{oc}(k)$ is the open circuit voltage.

Discretising the differential equation of the ECM leads to the discrete state space model,

$$\begin{bmatrix} V_1(k) \\ V_2(k) \end{bmatrix} = A \begin{bmatrix} V_1(k-1) \\ V_2(k-1) \end{bmatrix} + BI(k-1) \quad (2)$$

$$V_t(k) - V_{oc}(k) = C \begin{bmatrix} V_1(k) \\ V_2(k) \end{bmatrix} + DI(k) \quad (3)$$

where

$$A = diag(\mu_1, \mu_2), \quad B = [\,\rho_1 \;\; \rho_2\,]^T, \quad C = [\,1 \;\; 1\,], \quad D = [R]$$

with,

$$\mu_1 = exp(-\delta t/(R_1C_1)), \quad \rho_1 = R_1(1 - exp(-\delta t/(R_1C_1)))$$
$$\mu_2 = exp(-\delta t/(R_2C_2)), \quad \rho_2 = R_2(1 - exp(-\delta t/(R_2C_2)))$$

where $\delta t$ is the sampling time.

The details of this discretisation can be found in Tang et al. (2011) and references therein. Using (2) and (3) in (1) yields an auto regressive moving average (ARMA) model

$$V_t(k) = \theta_1 V_t(k-1) + \theta_2 V_t(k-2) + \theta_3 I(k) + \theta_4 I(k-1) + \theta_5 I(k-2) + \theta_6 + e(k) \quad (4)$$

where

$$\theta_1 = \mu_1 + \mu_2 \qquad \theta_4 = \rho_1 - \rho_2 - R(\mu_1 + \mu_2)$$
$$\theta_2 = -\mu_1\mu_2 \qquad \theta_5 = \mu_1\mu_2 R - \rho_1\mu_2 - \rho_2\mu_1$$
$$\theta_3 = R \qquad \theta_6 = (1 - (\mu_1 + \mu_2) + \mu_1\mu_2)V_{oc}. \quad (5)$$

Note, the open circuit voltage

$$V_{oc} = \theta_6/(1-\theta_1-\theta_2) \tag{6}$$

can be computed using the estimates of $\theta_1, \theta_2$ and $\theta_6$. Equation (4) can be written in the form

$$V_t(k) = \phi^T(k)\theta(k) + e(k), \tag{7}$$

where

$$\theta(k) = [\,\theta_1(k)\ \theta_2(k)\ \ldots\ \theta_6(k)\,]^T \tag{8}$$

and

$$\phi(k) = [V_t(k-1)\ V_t(k-2)\ I(k)\ I(k-1)\ I(k-2)\ 1]^T. \tag{9}$$

The parameters of a battery vary with time since the impedance of the battery changes with SOC (Illig et al. (2013)). To account this in (7) the parameter vector $\theta(k)$ is taken to be time varying (slowly time varying).

Estimation of $\theta(k)$ from (7) is a standard problem in system identification. If $\theta$ were a constant, then (7) can be rewritten in state space form as,

$$\theta(k+1) = \theta(k)$$
$$V_t(k) = \phi(k)\theta^T(k) + e(k). \tag{10}$$

Applying the Kalman filter to this model would yield an optimal state, $\widehat{\theta}(k+1)$, which are the estimates of the parameter $\theta(k)$. To track the time varying parameters, the state equation in (10) is modified to a random walk model.

$$\theta(k+1) = \theta(k) + v(k)$$
$$E(v(k)v^T(k)) = L, \tag{11}$$

where $E(\cdot)$ denotes the expected value and covariance matrix

$$L = \begin{pmatrix} \lambda_1 & 0 & \cdots & 0 \\ 0 & \lambda_2 & \cdots & 0 \\ \vdots & \vdots & \ddots & \vdots \\ 0 & 0 & \cdots & \lambda_6 \end{pmatrix} \tag{12}$$

is diagonal and positive definite. $\lambda_i$, which are the diagonal elements of $L$ determine how fast the parameters change with time. Smaller the value, slower the change. The $\lambda$'s are taken as tuning parameters and chosen such that the estimates of the output

$$\hat{V}_t(k) = \phi^T(k)\hat{\theta}(k-1) \tag{13}$$

are brought reasonably close to the true output (measured data $V_t(k)$).

The iteration steps of Kalman filter for the model (10) are

$$\hat{\theta}(k) = \hat{\theta}(k-1) + K(k)\epsilon(k) \tag{14}$$
$$\epsilon(k) = V_t(k) - \phi^T(k)\hat{\theta}(k-1) \tag{15}$$
$$K(k) = P(k-1)\phi(k)/[1+\phi^T(k)P(k-1)\phi(k)] \tag{16}$$
$$P(k) = P(k-1) - \frac{P(k-1)\phi(k)\phi^T(k)P(k-1)}{[1+\phi^T(k)P(k-1)\phi(k)]} + L. \tag{17}$$

For validating the $V_{oc}$ estimation, an HPPC test data (Tang et al. (2011)) is used. HPPC is a current profile having a discharging and a charging pulse with an interval of zero current in between. Here, a number of periodic HPPC pulses with a period of 140s is used. The width of the charge and discharge pulses are 10s each and their magnitude being $1.5C_b$. The zero current interval between the charge and the discharge pulses is 40s. The chosen values of the $\lambda$'s are given in Table 1. The voltage response $V_t$ corresponding to the HPPC input is shown in Fig. 2.

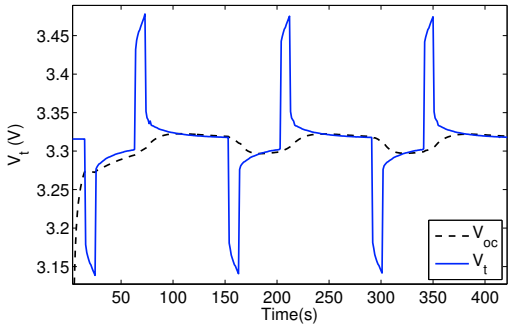


Fig. 2. $V_t$ and the estimated $V_{oc}$ for the HPPC input.

The $V_{oc}$, in (6) is obtained using the Kalman algorithm (17) by taking HPPC current profile as input and $V_t$ as output, is also plotted.

$V_t$ converges to $V_{oc}$ when the current flowing through the battery is zero and the battery is allowed to rest for sometime. Note, from the Fig. 2, $V_{oc}$ is converging to $V_t$ in the zero current intervals between discharging and charging pulses. Thus, validating the estimation. The ability of $V_{oc}$ to recover from a wrong initialisation can also be observed at the initial intervals in Fig. 2.

### *4.2 SOC estimation*

*Hysteresis phenomenon in Lithium ion batteries:* The $LiFePO_4$ battery is known to show hysteresis behavior (Roscher and Sauer (2011)), leading to a one-to-many mapping from SOC to $V_{oc}$. In such a situation, a proper hysteresis model is necessary for estimating the SOC from the $V_{oc}$.

The hysteresis effect of the battery is captured by carrying out a charge - discharge cycle from 0% SOC ($V_t$ = 2.8V) to 100% SOC ($V_t$ = 3.6V) and back to 0% SOC. A very low value of current ($C_b/20$) is used to ensure that $V_{oc}$ is approximately equal to $V_t$. Since a constant current is applied, the SOC is assumed to be increasing at a constant rate between 0 and 1, when the $V_t$ varies from 2.8V to 3.6V. Similarly, while discharging with same constant current, the SOC decreases at a constant rate from 1 to 0 with $V_t$ varying from 3.6V to 2.8V. This experiment yields $V_{oc}$-SOC curves which follow separate paths for charging and discharging as shown in Fig. 3. These curves together constitute the major loop of the hysteresis. For modeling the hysteresis behavior, Chebyshev polynomials of degree 14 are fit to the charging and discharging curves plotted in Fig. 3. The fitted curves along with the actual hysteresis data, are shown in the Fig. 3. The Chebyshev polynomial fits for the charging and the discharging curves are denoted by $P_{ch}(x)$ and $P_{dch}(x)$ respectively. During normal operations of a battery, the $V_{oc}$ can attain any value within the boundaries of the hysteresis loop. This value depends on its past value and the direction of the current $I$. To capture this behavior, $V_{oc}^k$ ($V_{oc}$ at time instant $k$) is written as in Roscher and Sauer (2011),

Table 1. The tuned forgetting factor values.

| $\lambda_1$ | $\lambda_2$ | $\lambda_3$ | $\lambda_4$ | $\lambda_5$ | $\lambda_6$ |
|---|---|---|---|---|---|
| 0.02 | 0.001 | 0.001 | 0.0001 | 0.0001 | 0.0001 |

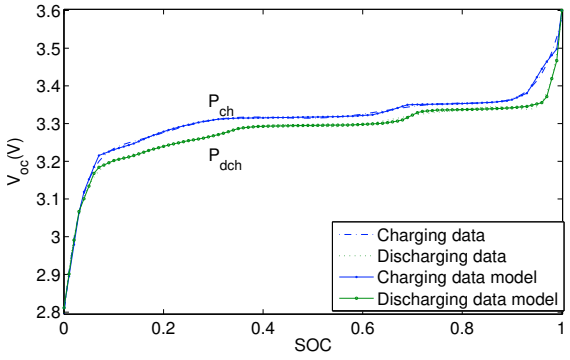


Fig. 3. Chebyshev polynomial model of hysteresis.

$$V_{oc}^k(SOC, \psi) = \psi P_{ch}^k(SOC) + (1-\psi)P_{dch}^k(SOC) \quad (18)$$

where $\psi \in [0,1]$ is a weighing constant and $SOC \in [0,1]$. Here, $\psi = 1$ and $\psi = 0$ are two special cases when the $V_{oc}$ meets the upper and lower boundaries respectively. When $0 < \psi < 1$, the $V_{oc}$ can be anywhere within the loop forming the minor curves of hysteresis as shown in Fig. 4. Once the $V_{oc}$ is estimated at an instant $k$, estimation of the corresponding values of SOC and $\psi$ is posed as a non-linear Kalman filtering problem. A constrained unscented Kalman filter (CUKF) (Teixeira et al. (2010)), is used for the SOC estimation.

*State Space Model of Hysteresis:* The $SOC_k$ and $\psi_k$ follow the state equations,

$$SOC_{k+1} = SOC_k - \eta(I_k \delta t)/C_b \quad (19)$$
$$\psi_{k+1} = \psi_k - (I_k \delta t)/C_{hys} \quad (20)$$

respectively.

Here $C_b$ is the capacity of the lithium ion cell, $I_k$ is the current at instant $k$ and $\delta t$ is the discrete time interval. $\eta$ is a constant known as coulombic efficiency, which accounts for the loss during charging and discharging. $\eta$ for charging and discharging states are separately denoted as $\eta_c$ and $\eta_d$, where $\eta_c \in [0,1]$ and $\eta_d > 1$. For example, if $\eta_c = 0.98$ for charging and $\eta_d = 1.02$ for discharging indicates 2% loss during both charging and discharging.

The value of $V_{oc}$ in hysteresis minor branch is obtained using (18). The transition of $V_{oc}$ between the hysteresis major curves, see Fig. 4, occurs when the direction of current changes. The direction of the transition depending on sign of current $I_k$ and the past value of $V_{oc}$. $C_{hys}$ represents the change in capacity during such a transition, see Fig. 4. The value of $C_{hys}$ depends on the current value of SOC and roughly varies from $0.1C_b - 0.3C_b$. Since the accurate value of $C_{hys}$ may vary as battery ages and is difficult to map along all values of SOC, an average value of $0.2C_b$ is used in state prediction equation . From (18), (19) and (20), the state space model for hysteresis can be written as

$$\begin{aligned} x_{k+1} &= Ax_k + Bu_k + w_k \\ y_k &= f(x_k, u_k) + v_k \end{aligned} \quad (21)$$

where, $x_k$ is the state vector $[SOC_k \quad \psi_k]^T$, $u_k$ is the current $I(k)$, $A$ is a $2 \times 2$ identity matrix, Matrix B $= [\, \delta t/C \;\; \delta t/C_{hys}\,]^T$, output vector $y_k$ is $V_{oc}$, and $f(\cdot)$ is the non-linear function (18). $w_k$ and $v_k$ are process noise and measurement noise respectively, which are assumed

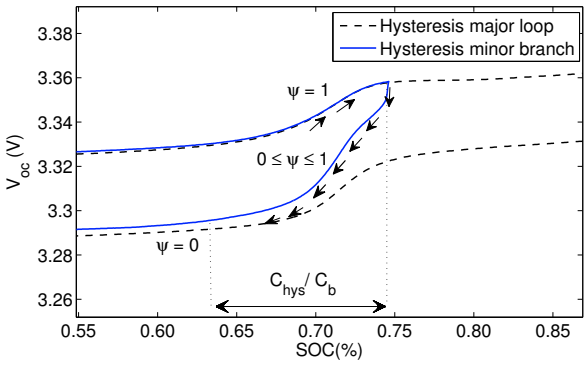


Fig. 4. Hysteresis minor branch.

to be Gaussian random variable (GRV) of zero mean with covariance matrices denoted by $Q'$ and $R'$, where,

$$Q' = \sigma_q^2 \begin{bmatrix} 1 & 0 \\ 0 & 1 \end{bmatrix}, \; R' = \sigma_r^2. \quad (22)$$

Here, $\sigma_q$ and $\sigma_r$ are taken as tuning parameters. $\sigma_q = 0.14$ and $\sigma_r = 0.07$ were found to be giving the best results. Since the Chebyshev polynomials are defined in [-1,1], SOC is normalised within this interval.

Using CUKF the values of SOC and $\psi$ are estimated from the state space model (21).

### *4.3 UKF and the concept of sigma points*

UKF is a nonlinear Kalman filter which has the ability to avoid filtering errors generated by linearisation of a nonlinear model. See (Julier and Uhlmann (1997)). In UKF, a set of deterministic vectors- known as sigma points, are generated from the current state vector. These vectors are distributed around the mean state vector in accordance with its variance. The sigma points are propagated through the non-linear process model (21) and the mean and variance of the transformed state vector is recovered from these transformed sigma points. Using this method, the true statistics of the transformed state vector are determined. The sigma points are obtained using a method called unscented transform (UT) which is explained in section 4.3.1.

In CUKF, the sigma points are generated such that the states are restricted within certain limits. This will make the estimation bounded compared with a standard UKF.

*Unscented Transform for CUKF:* Assume, the state vector $x_k$ is having a mean $\hat{x}_k$ and covariance matrix $P_k^{xx}$. For a state vector of dimension $n$, minimum $2n+1$ sigma points are required to capture its statistics. Since $x_k \in R^2$, in (21), 5 sigma points denoted by $X_{j,k}$, where $X_{j,k} \in R^2$, $j = 0....2n$ and their weights $\gamma$, where $\gamma \triangleq [\gamma_0 ... \gamma_{2n}]_{1\times 2n+1}$ have to be generated. Sigma points and their corresponding weights should satisfy the conditions

$$\sum_{j=0}^{2n} \gamma_j X_{j,k} = \hat{x}_k, \quad \sum_{j=0}^{2n} \gamma_j = 1,$$
$$\sum_{j=0}^{2n} \gamma_j [X_{j,k} - \hat{x}_k][X_{j,k} - \hat{x}_k]^T = P_k^{xx},$$

and $\gamma_j \geq 0$, for all $j = 0, 1, \ldots, 2n$. Since, SOC and $\psi$ are confined in the interval $[0, 1]$, all sigma points have to be restricted between the lower and upper limit: $[0, 0]^T$ and $[1, 1]^T$ denoted by $d_k$ and $e_k$ respectively. So, a method called interval constrained unscented transform (ICUT) (Teixeira et al. (2010)) is used to generate the sigma points which confirms to the inequality $d_k \leq \hat{x}_k \leq e_k$.

The sigma point matrix $X_k$ consisting of the sigma point vectors $X_{j,k}$, are generated by,

$$X_k = \hat{x}_k \left[ 1 \ 1 \ \ldots \ 1 \right]_{1\times 2n+1} + \left[ 0_{n\times 1} \ M_{k(n\times 2n)} \right] \quad (23)$$

where,

$$col_j(M_k) = \begin{cases} \min(col_j(\Theta_k)) col_j[(P_k^{xx})^{\frac{1}{2}}], & j = 1 \ldots n \\ -\min(col_j(\Theta_k)) col_j[(P_k^{xx})^{\frac{1}{2}}], & j = n+1 \ldots 2n. \end{cases} \quad (24)$$

Here $col_j(\cdot)$ is the $j^{th}$ column of a matrix and $\min(\cdot)$ represents the element having the minimum value in a vector.

For $i = 1 \ldots n$ and $j = 1 \ldots 2n$,

$$\Theta_{i,j,k} = \begin{cases} \sqrt{n+\lambda}, & S_{i,j,k} = 0 \\ \min\left(\sqrt{n+\lambda}, \frac{(e_{i,k}-\hat{x}_{i,k})}{S_{i,j,k}}\right), & S_{i,j,k} > 0 \\ \min\left(\sqrt{n+\lambda}, \frac{(d_{i,k}-\hat{x}_{i,k})}{S_{i,j,k}}\right) & S_{i,j,k} < 0 \end{cases} \quad (25)$$

and,

$$S_k = \left[ \ (P_k^{xx})^{\frac{1}{2}} \ -(P_k^{xx})^{\frac{1}{2}} \ \right]_{2\times 2n}. \quad (26)$$

Here $\lambda > -n$, which needed to be tuned. $\lambda$ decides the spread of sigma points around the mean and $\lambda = -0.42$ was found to be giving the best result.

The weights $\gamma_{j,k}$ can be calculated by,

$$\gamma_{j,k} = \begin{cases} b_k, & j = 0 \\ a_k \min(col_j(\Theta_k)) + b_k, & j = 1 \ldots 2n \end{cases} \quad (27)$$

where,

$$a_k = \frac{2\lambda - 1}{(2(n+\lambda)(\sum_{j=1}^{n} \min(col_j(\Theta_k)) - (2n+1)(\sqrt{n+\lambda}))} \quad (28)$$

$$b_k = \frac{1}{2(n+\lambda)} - a_k\sqrt{(n+\lambda)} \quad (29)$$

The above procedure, which generates $X_k$ and $\gamma_k$ from $x_k, P_k^{xx}, e, d, n$, and $\lambda$ is denoted by,

$$[\gamma_k, X_k] \triangleq \beta_{ICUT}(\hat{x}_k, P_k^{xx}, e, d, n, \lambda). \quad (30)$$

*CUKF algorithm*

*Step 1: Initialisation.* The Kalman gain ($K_k$), process covariance matrix ($P_k^{xx}$) and states $x_k = [S_k, \psi_k]^T$ are set to their respective initial values. $K_0$ is given an arbitrary positive value. Approximate values for $S_0$ and $\psi_0$ can be usually obtained from their last states. $P_0^{xx}$ is usually set as a positive definite matrix having elements with reasonably high values. Here, the initial values are taken as,

$$P_0^{xx} = \begin{bmatrix} 10^3 & 0 \\ 0 & 10^3 \end{bmatrix}, K_0 = \left[10^3, 10^3\right], \begin{bmatrix} S_0 \\ \psi_0 \end{bmatrix} = \begin{bmatrix} 0 \\ 1 \end{bmatrix}. \quad (31)$$

*Step 2: Sigma point generation using ICUT.* Sigma points corresponding to the state $\hat{x}_{k-1|k-1}$ and their weights are derived as,

$$[\gamma_{k-1}, X_{k-1|k-1}] \triangleq \beta_{ICUT}(\hat{x}_{k-1|k-1}, P_{k-1|k-1}^{xx}, e, d, n, \lambda) \quad (32)$$

where $e$ and $d$ are $[1, 1]^T$ and $[0, 0]^T$ respectively.

*Step 3: State prediction.* Each of these sigma points are applied to the state prediction equation in (21) to get the corresponding apriori transformed sigma points.

$$X_{j,k|k-1} = AX_{j,k-1|k-1} + BU_{k-1}, j \in 0..2n. \quad (33)$$

The mean of the apriori state is calculated from transformed sigma points and their weights using the formula,

$$\hat{x}_{k|k-1} = \sum_{j=0}^{2n} \gamma_j X_{j,k-1}. \quad (34)$$

Using the weighted mean, forecast error covariance matrix can be found,

$$P_{k|k-1}^{xx} = \sum_{j=0}^{2n} \gamma_j [X_{j,k|k-1} - \hat{x}_{k|k-1}] \left[X_{j,k|k-1} - \hat{x}_{k|k-1}\right]^T + Q' \quad (35)$$

where $Q'$ is as in (22).

*Step 4: Updating the sigma points and their weights.*

$$\left[\gamma_k, X_{k|k-1}\right] = \beta_{ICUT}(\hat{x}_{k|k-1}, e, d, P_{k|k-1}^{xx}, n, \lambda). \quad (36)$$

*Step 5: Generating the output vector.* Output vectors for each sigma point

$$Y_{j,k|k-1} = f\left(X_{j,k|k-1}\right). \quad (37)$$

Mean output is,

$$\hat{y}_{k|k-1} = \sum_{j=0}^{2n} \gamma_j . Y_{j,k|k-1}. \quad (38)$$

Here, $\hat{y}_{k|k-1}$ is the estimated terminal voltage $\hat{V}_t(k|k-1)$ calculated from the predicted states.

*Step 6: Generating the covariance matrices.* Innovation covariance matrix is derived as,

$$P_{k|k-1}^{yy} = \sum_{j=0}^{2n} \gamma_j [Y_{j,k|k-1} - \hat{y}_{k|k-1}] \left[Y_{j,k|k-1} - \hat{y}_{k|k-1}\right]^T + R' \quad (39)$$

where $R'$ is taken as per (22).

Cross covariance matrix is obtained as,

$$P_{k|k-1}^{xy} = \sum_{j=0}^{2n} \gamma_j [X_{j,k|k-1} - \hat{x}_{k|k-1}] \left[Y_{j,k|k-1} - \hat{y}_{k|k-1}\right]^T \quad (40)$$

*Step 7: Data assimilation.* Kalman gain matrix is calculated

$$K_k = P_{k|k-1}^{xy} \left(P_{k|k-1}^{yy}\right)^{-1}. \quad (41)$$

Posteriori sigma points are obtained as,

$$X_{j,k|k} = X_{k|k-1} + K_k(y_k - Y_{j,k|k-1}) \quad (42)$$

where the $y_k$ is the measured $V_t(k)$.
Posteriori mean state vector is calculated as,

$$\hat{x}_{k|k} = \sum_{j=0}^{2n} \gamma_j X_{j,k|k}. \quad (43)$$

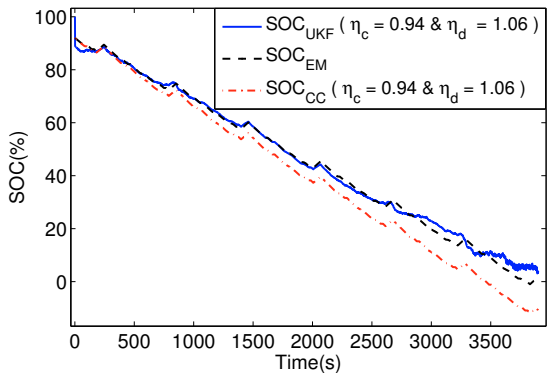


Fig. 5. Comparison of SOCs from estimation ($SOC_{UKF}$), simulation ($SOC_{EM}$) and coulomb counting ($SOC_{CC}$)

Posteriori covariance matrix is calculated as,

$$P^{xx}_{k|k} = \sum_{j=0}^{2n} \gamma_j [X_{j,k|k-1} - \hat{x}_{k|k-1}][X_{j,k|k-1} - \hat{x}_{k|k-1}]^T. \quad (44)$$

The above steps are repeated for each instance of k. Irrespective of the initial values, the SOC, which is the first element of $x_k$, will converge to its true value after a few iterations.

## 5. PERFORMANCE AND ERROR ANALYSIS

A current profile [1] that simulates a typical dynamic charge - discharge scenario in HEVs was used used to study the performance of the algorithm. To determine the actual SOC corresponding to the current profile, a full electrochemical model (EM) of the battery (ANR26650M1A) is simulated using COMSOL [2] software. A 1D isothermal model is used and the SOC obtained from the simulation is denoted by $SOC_{EM}$.

The state prediction equation (19) of the UKF algorithm uses an approximate value of $\eta$ for predicting $\text{SOC}_{k+1}$ from $\text{SOC}_k$. Irrespective of the value of $\eta$ used in the (19), the final estimated SOC by UKF is expected to follow the $SOC_{EM}$.

The $SOC_{CC}$ profiles for $\eta = (0.94, 1.06)$ is plotted in Fig. 5 along with $SOC_{UKF}$ and $SOC_{EM}$. Here, $SOC_{UKF}$ can be seen following $SOC_{EM}$ even though the state prediction equation in UKF algorithm uses $\eta = (0.94, 1.06)$.

## 6. CONCLUSION

A $LiFePO_4$ battery was modeled as an equivalent circuit. An HPPC current profile was applied to the battery and the corresponding terminal voltages were recorded as the output. From this input-output data, the estimation of the circuit elements and the open circuit voltage $V_{oc}$ were posed as a Kalman filtering problem.

In order to determine the hysteresis curves relating the SOC and the open circuit voltage $V_{oc}$, the battery was charged and discharged at a very low current. As the current was very low, the terminal voltage $V_t$ was taken to be equal to $V_{oc}$. Furthermore, as losses are minimal at low currents, SOC was calculated by coulomb counting. The resulting non-linear curves between $V_{oc}$ and SOC were taken as the major loop of hysteresis.

Minor branches of the hysteresis appear when the battery is switched between charging and discharging modes. Minor branches were modeled as a weighted linear combination of major curves. This model was non-linear, in the weighting coefficients and SOC. An Unscented Kalman Filter (UKF) with states constrained between 0 and 1 was used to estimate the SOC.

The estimated SOC was compared with the SOC obtained using a full electrochemical model from COMSOL. The $\eta$ in the UKF algorithm was varied and resulting SOC estimations were compared with the simulated SOC.

[1] http://tinyurl.com/o79vb2a
[2] http://www.comsol.com

## REFERENCES

Illig, J., Schmidt, J.P., Weiss, M., Weber, a., and Ivers-Tiffée, E. (2013). Understanding the impedance spectrum of 18650 LiFePO4-cells. *J. Power Sources*, 239, 670–679.

Julier, S.J. and Uhlmann, J.K. (1997). New extension of the kalman filter to nonlinear systems. *Proc. SPIE*, 3068, 182–193.

Lim, K., Ayad, H., Duong, V.h., Wai, K., Zhang, P., and Xue, S. (2016). Fading Kalman filter-based real-time state of charge estimation in LiFePO 4 battery-powered electric vehicles. *Applied Energy*, 169, 40–48.

Prada, E., Di Domenico, D., Creff, Y., Bernard, J., Sauvant-Moynot, V., and Huet, F. (2012). Simplified Electrochemical and Thermal Model of LiFePO4-Graphite Li-Ion Batteries for Fast Charge Applications. *J. Electrochem. Soc.*, 159(9), A1508–A1519.

Roscher, M.a. and Sauer, D.U. (2011). Dynamic electric behavior and open-circuit-voltage modeling of LiFePO4-based lithium ion secondary batteries. *J. Power Sources*, 196(1), 331–336.

Tang, X., Mao, X., Lin, J., and Koch, B. (2011). Li-ion battery parameter estimation for state of charge. In *American Control Conference (ACC), 2011*, 941–946.

Teixeira, B.O., a.B. Tôrres, L., Aguirre, L.a., and Bernstein, D.S. (2010). On unscented Kalman filtering with state interval constraints. *J. Process Control*, 20(1), 45–57.